



Investigating drought over the Central Highland, Vietnam, using regional climate models



Vu Minh Tue^{a,c,d}, Srivatsan V. Raghavan^{a,c,d,*}, Pham Duc Minh^a, Liong Shie-Yui^{a,b,c,d}

^a Tropical Marine Science Institute, National University of Singapore (NUS), Singapore

^b Willis Research Network, Willis Re Inc., London, United Kingdom

^c Center for Environmental Modeling and Sensing, SMART, Singapore

^d Center for Hazards Research, Dept. of Civil and Environmental Engineering, NUS, Singapore

ARTICLE INFO

Article history:

Available online 15 November 2014

Keywords:

Droughts
Regional climate models
SPI
Climate change

SUMMARY

The Standardized Precipitation Index (SPI) has been computed based on the monthly precipitation for different observed and modelled datasets over the Central Highland, Vietnam during the period 1990–2005. Station data from a total of 13 stations were collected from the study region and used for benchmarking to compare gridded observation data and two regional climate models (RCMs). Various characteristics of drought across the study region were analyzed using spatial and temporal distributions, number of drought events, their frequency and their deficit. The RCMs were able to capture the SPI temporal distributions of station data fairly well. The analysis from RCMs showed close estimation for the number of drought events to station data and gridded observations. In terms of Drought Deficit and frequency, the RCMs matched the station data better than gridded observations. The drought trend was carried out using a Modified Mann–Kendall trend test which yielded no clear trends that suggested the need for longer records of data. The results also highlight uncertainties in gridded data and the need for robust station data quality and record lengths. The regional climate models proved to be appropriate tools in assessing drought over the study area as they can serve as good proxies over data sparse regions, especially in developing countries, for studying detailed climate features at sub regional and local scales.

© 2014 Elsevier B.V. All rights reserved.

1. Introduction

Drought is a natural feature of the climate cycle that quietly wreaks havoc in most regions of the globe (American Meteorological Society, 2013). The United States Environment Protection Agency (EPA) also listed severe drought as a natural disaster (USEPA website). In the statistics of natural disasters by Obasi (1994), the World Meteorological Organization (WMO) has observed that during 1967–1991, drought accounted only for 7.3% of all events for all type of natural disasters but it led to 38% number of people killed, one of the highest among all natural hazards. Drought affects natural habitats, ecosystems and many economic and social sectors, from the foundation of civilization – agriculture – to transportation, urban water supply and the modern complex industries (Heim, 2002). Understanding drought and modelling its components have drawn the attention of ecologists,

hydrologists, meteorologists and agricultural scientists (Mishra and Singh, 2011).

A common tool utilized to monitor current drought conditions is a drought index expressed by a numeric number, which is believed to be far more functional than raw data during decision-making (Belayneh and Adamowski, 2012). Two widely used indices for drought are the Palmer Drought Severity Index (Palmer, 1965) and the Standardized Precipitation Index (McKee et al., 1993). The PDSI requires information such as precipitation, temperature and available water content from soil to study the wet and dry conditions using water balance technique. Guttman (1999) strongly suggested that users of the Palmer indices consider the Standardized Precipitation Index (SPI) as either a primary drought index or as an equal companion to the Palmer indices. Applying SPI requires only monthly precipitation data to yield a better representation of abnormal wetness and dryness, than using PDSI which is more demanding in terms of ground data and hence problematic in regions where good ground data do not exist.

The SPI is both a standardized index and a probabilistic drought index. Standardization of a drought index ensures independence from geographical position as the index in question is calculated

* Corresponding author at: Tropical Marine Science Institute, National University of Singapore (NUS), Singapore. Tel.: +65 65163081; fax: +65 67761455.

E-mail address: tmsvs@nus.edu.sg (S.V. Raghavan).

with respect to the average precipitation (Bordi and Sutera, 2007). The SPI is considered as the most appropriate index for monitoring the variability of droughts since it is easily adapted to local climate, has modest data requirements and can be computed at almost any time scale (Ntale and Gan, 2003). In Asia, many researches have adapted SPI as an effective tool for their countries' drought monitoring. Yusof et al. (2014) applied SPI to assess rainfall characteristic over Peninsular Malaysia and concluded that the whole peninsula is predicted to have an increasing trend during drought events. Zhang et al. (2014) used SPI of 3 months to monitor winter wetness and dryness in Southeast China. Vu et al. (2013) also compared SPI with the de Martonne J index (de Martonne, 1926) and the Ped index (Ped, 1975) to monitor drought for the whole Vietnam from 50 meteorological stations. Lyon et al. (2009) evaluated drought in Sri Lanka using 3, 6, 9 and 12-month cumulative drought index SPI and found out the 9-month SPI provided the strongest relationships overall. In the "Lincoln Declaration on Drought Indices", 54 experts from all regions agreed on the use of a universal meteorological drought index for more effective drought monitoring and climate risk management (WMO, 2009). Thus, experts participating in the Inter-Regional Workshop on Indices and Early Warning Systems for Drought, held at the University of Nebraska-Lincoln, USA in 2009, made a significant step through a consensus agreement that the SPI should be used to characterize meteorological droughts by all National Meteorological and Hydrological Services around the world (WMO, 2009). To this end, this study makes use of the results from a Regional Climate Model and SPI index to assess drought over a climate vulnerable region in Vietnam.

2. Study region

The study region is the Central Highland of Vietnam, which is located southeast of the Indochina Peninsula, between longitudes 11°N to 15°N and latitudes 107°E to 109°E. The region has complex topography: (1) high mountains that range from 1000 m to 2500 m, located in the northeast and in the southeast of the study region. (2) Plateau topography is most prominent spreading westerly from Da Lat highland (1000 m) to the border with Cambodia (100 m). (3) Valley topography with a small area lying over western side of the region, distributed along the river basin (shown in Fig. 1).

The soil in the study region has 1.7 million ha of basaltic area (comprising 90% total basaltic area in Vietnam) and 3 million ha of forest (22% total forested land). Therefore, the region is suitable for planting perennial plants like coffee, rubber or annual plants like cocoa, pepper, sugar cane and cashew. The cultivated area is about 800,000 ha with major crops in the region. Coffee is the most important crop in the Central Highland and Vietnam is the world's second largest coffee exporter after Brazil.

The population is about four million people and 80% of the population live in rural and mountainous areas. Two main tributaries of the Mekong river also come from this region: Sesan and Srepok, which serve as the main source of water supply for agricultural activities. The total annual rainfall ranges from 1500 to 2400 mm. Rainy season occurs from May to October which account for 80% of the annual rainfall. Dry season is from November to the following year April that coincides with winter–spring crop seasons.

With climate change, the frequency and magnitude of droughts are very likely to increase and the poor nations are very vulnerable to such changes (IPCC, 2014). Vietnam is prone to drought in addition to being susceptible to floods. The climate in Vietnam is strongly affected by monsoons and its complex topography. The total precipitation amount in the dry season accounts for

approximately 15–25% of the annual precipitation. There are limited statistical figures of sectors affected by drought events since the 1980s in Vietnam. During the 1997–1998 El Niño event, most regions in Vietnam, especially regions from central to south, were significantly affected by severe drought. According to a drought assessment by the Ministry of Agriculture and Rural Development (MARD), Vietnam, in 1997–1998, about three million people were affected and the total losses in terms of agricultural production were estimated to be about 400 million US dollars. The country being so vulnerable, very few studies on droughts have been made over Vietnam (Vu et al., 2013; Dao, 2002; Nguyen, 2005). In Vietnam, the Central Highland area is important for perennial plantation and has been known to be largely drought prone. The Central Highland suffers from severe drought. Nguyen et al. (2007) found that the precipitation in Central Highland, during October, November and April, is highly related to the El Niño Southern Oscillation (ENSO). Nguyen (2005) characterized drought over the Central Highland whose studies pointed out that 1998 and 2005 were the two typical severe drought events over this region, especially during the winter–spring crop season. A study by Dao (2002) indicated a series of drought events in this area from 1994 to 1998 during the winter–spring season. Tran (1999) pointed out that the wide spread drought in 1997–1998 was related to a strong El Niño year. In a recent study comparing different drought indices for Vietnam, Vu et al. (2013) suggested that no particular meteorological drought indices would be the best to represent the drought conditions in Vietnam and it remains a challenge to better understand the relationship between drought and climate. This study, therefore, attempts to assess the regional climate model's ability to simulate drought characteristics over this region, so that future drought conditions using the model can be assessed with more confidence.

3. Methodology, model and data

3.1. Drought characterization indices

3.1.1. Standardized Precipitation Index (SPI)

The SPI was first introduced by McKee et al. (1993) by analyzing historical monthly precipitation. A set of averaging periods are selected on a moving window basis to determine a set of time scale of period 'i' months ($i = 3, 6, 12, 24, 48$). A 3-month SPI can be very effective in showing seasonal trends in precipitation while SPI 12 reflects long-term precipitation patterns (Belayneh and Adamowski, 2012). In this study $i = 12$ is selected in order to assess meteorological drought because it is more suitable for water resources management purposes (Raziei et al., 2009) and more appropriate for identifying the persistence of dry periods (Gocic and Trajovic, 2013; Tabari et al., 2012). Each dataset is fitted to the Gamma distribution that has the probability density function as:

$$g(x) = \frac{1}{\beta^\alpha \Gamma(\alpha)} x^{\alpha-1} e^{-x/\beta}, \quad \text{for } x > 0 \quad (1)$$

where $x > 0$ is the amount of accumulated precipitation. Based on each data set, a set of shape parameter $\alpha > 0$ and shape parameter $\beta > 0$ is estimated. $\Gamma(\alpha)$ is the Gamma function that is defined by the integral:

$$\Gamma(\alpha) = \int_0^\infty y^{\alpha-1} e^{-y} dy \quad (2)$$

After estimating coefficients α and β , an expression for the cumulative probability $G(x)$ can be obtained that represents a certain amount of rain that is observed for a given month at time scale i :

$$G(x) = \int_0^\infty g(x) dx \quad (3)$$

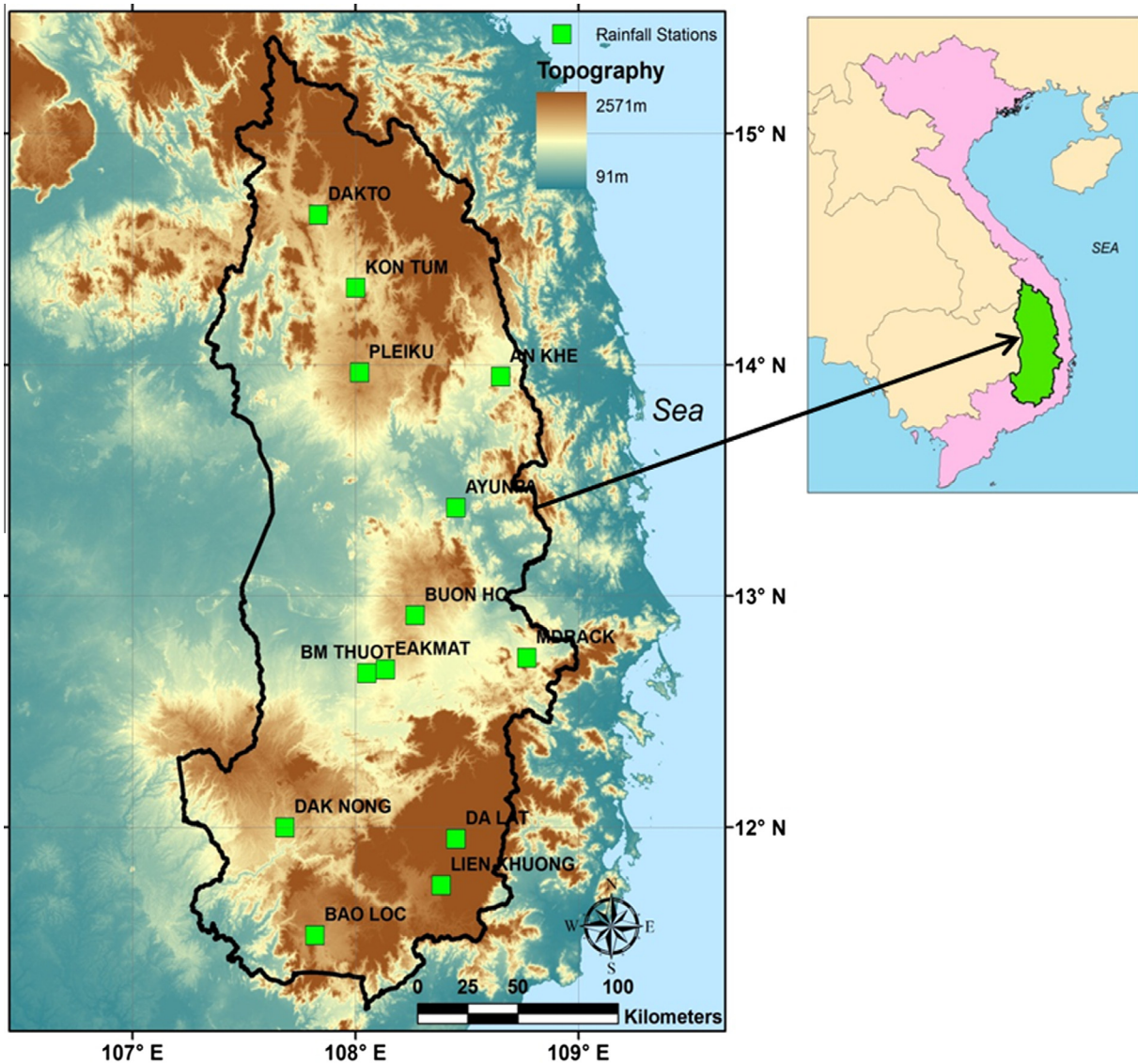


Fig. 1. Central Highland, Vietnam – topography and rainfall stations.

However, the Gamma function is not defined by $x = 0$, and there may be no precipitation. If q is the probability of zero precipitation, the cumulative probability of precipitation $H(x)$ observed is computed using:

$$H(x) = q + (1 - q)G(x) \quad (4)$$

The cumulative probability $H(x)$ is then transformed into a normal standard distribution with mean $\mu = 0$ and standard deviation $\sigma = 1$ from which we obtain SPI. The SPI is the inverse of the normal cumulative distribution function at the corresponding probability $H(x)$.

Wu et al. (2005) simulated the effect of the SPI data record length by examining correlation coefficients, index of agreement and consistency of dry/wet between SPI values derived from different precipitation record lengths. They concluded that the SPI computed from different length of record are highly correlated and consistent when the gamma distribution of precipitation over the different time periods is similar. Therefore, in this study, in order to overcome our limitation of having only a short record of 16 years from 1990 to 2005, we did a sensitivity analysis using 2 stations (Buon Me Thuot and Pleiku) which have the longest record from 1961 to 2007 (47 years), located at the south and north of the

domain (Fig. 1 and Table 1). To enable a better comparison of the gridded data, we use bi-linearly interpolated APH data (see Section 3.2.4) (to the station point locations) for the same period. The correlation coefficients between the SPI values derived from the long record 1961–2007 and the 2 short records 1990–2005 (16 years) and 1998–2005 (8 years) are shown in Table 2. As seen, the correlation coefficients between SPI derived from 47 years and 16 years for STA (see Section 3.2.4) and APH are quite high at 0.997 and 0.994, respectively, for both stations. The correlation coefficients of SPI values between 47 years and 8 years are lower, at about 0.99 for Buon Me Thuot and at 0.95 for Pleiku. We, hence, assume that the 16 and 8 years records are able to derive the SPI values for the study region, given the high correlation coefficient with 47 years data. The limitation of using a short data record for this region is, therefore, overcome. The drought classification based on SPI adapted from McKee et al. (1993) is shown in Table 3.

3.1.2. Trend analysis by Modified Mann–Kendall test

The trend analysis is assessed using the Mann–Kendall (MK) trend test, developed by Mann (1945), Kendall (1975). Mann–Kendall test has been widely used in numerous analyses of trends in hydrologic data and applications (Douglas et al., 2000); trends

Table 1
Name of rainfall station used in study.

No	Name	Lon	Lat	Start	End
1	Bao Loc	107.82	11.53	1962	2007
2	Lien Khuong	108.38	11.75	1981	2007
3	Da Lat	108.45	11.95	1964	2007
4	Dak Nong	107.68	12.00	1978	2007
5	Buon Me Thuot	108.05	12.67	1961	2007
6	Eakmat	108.13	12.68	1979	2007
7	MDrack	108.77	12.73	1977	2007
8	Buon Ho	108.27	12.92	1982	2007
9	Ayunpa	108.45	13.38	1979	2007
10	An Khe	108.65	13.95	1978	2007
11	Pleiku	108.02	13.97	1961	2007
12	Kon Tum	108.00	14.33	1964	2007
13	Dak To	107.83	14.65	1981	2007

Table 2
Sensitivity study between SPI values derived from long and short period for two stations and two datasets.

Original period	1961–2007			
Correlated with	1990–2005		1998–2005	
Dataset	STA	APH	STA	APH
Buon Me Thuot	0.997	0.993	0.993	0.991
Pleiku	0.997	0.994	0.943	0.953

Table 3
Drought classification [adopted from McKee et al. (1993)].

SPI values	Drought category
0 to -0.99	Mild drought
-1.00 to -1.49	Moderate drought
-1.50 to -1.99	Severe drought
<-2.00	Extreme drought

analyses of precipitation (Partal and Kahya, 2006; Tabari and Talae, 2011b; Gocic and Trajovic, 2013); trends analyses of temperature (Tabari and Talae, 2011a; Gocic and Trajovic, 2013); trends analyses of flood and low flows (Douglas et al., 2000) and those of streamflow (Birsan et al., 2005; Novotny and Stefan, 2007).

3.1.2.1. The effect of serial correlation of Mann–Kendall trend test.

As Mann–Kendall test is a non-parametric test, it does not require the data to be distributed normally. However, the SPI values are calculated on a moving average window of accumulation, hence it has a serial correlation effect that may not be applied directly by the MK trend. In order to overcome this, a method suggested by Hamed and Rao (1998) to modify the Mann–Kendall trend has been applied. In this paper, we name it as ‘MMK trend test’. The MMK was modified by considering the lag-*i* autocorrelation in the stations. This method has been applied effectively in Daufresne et al. (2009) to study of trends in hydro-meteorological series and to detect SPI trend in Zhang et al. (2012). The following methodology briefly shows the procedure of MMK.

Assume that we have a data set ($X = x_1, x_2, \dots, x_n$) that is a sample of *n* independent and identically distributed random variables. The distributions of x_k and x_j are not identical for all $k, j \leq n$ with $k \neq j$ which suggests that not all of data points have the same value. The data values are ranked as an ordered time series and each data value is compared with all subsequent data values. In other words, each data value is treated as a reference and is compared to all data that follow in time. To compare two data samples x_j and x_k , a test statistic Kendall’s *S* (Kendall, 1975) is calculated as:

$$S = \sum_{k=1}^{n-1} \sum_{j=k+1}^n \text{sgn}(x_j - x_k) = \begin{cases} +1 & \text{if } (x_j - x_k) > 0 \\ 0 & \text{if } (x_j - x_k) = 0 \\ -1 & \text{if } (x_j - x_k) < 0 \end{cases} \quad (5)$$

where *n* is the number of data points that should be larger than 10. The variance of *S* is computed using:

$$\text{Var}(S) = \frac{[n(n-1)(2n+5)]}{18} \quad (6)$$

Hamed and Rao (1998) found that the variance of *S* is biased when significant temporal autocorrelations exist in a time series. In order to overcome this, they introduced the correction ratio n/n_s^* due to autocorrelation in the data, in which, the new variance of *S* is:

$$\text{Var}^*(S) = \text{Var}(S) \frac{n}{n_s^*} \quad (7)$$

And the autocorrelation correction is computed by:

$$\frac{n}{n_s^*} = 1 + \frac{2}{n(n-1)(n-2)} \sum_{i=1}^{n-1} (n-i)(n-i-1)(n-i-2)\rho_s(i) \quad (8)$$

where *n* is the actual number of observation and $\rho_s(i)$ is the autocorrelation function of the ranks of the observations. The significant trend is tested by the *Z* index using the relation:

$$Z = \begin{cases} \frac{S-1}{\sqrt{\text{Var}(S)}} & \text{if } S > 0 \\ 0 & \text{if } S = 0 \\ \frac{S+1}{\sqrt{\text{Var}(S)}} & \text{if } S < 0 \end{cases} \quad (9)$$

Positive values of *Z* in Eq. (9) indicate increasing trends (upward trend) while negative *Z* indicate decreasing trends (downward trend). When testing either increasing or decreasing monotonic trends at the α significance level, the null hypothesis was rejected for an absolute value of *Z* greater than $Z_{1-\alpha/2}$ that is obtained from the standard normal cumulative distribution tables (Tabari and Talae, 2011b; Gocic and Trajovic, 2013). In this paper, at a significance level of $\alpha = 0.05$, the trend detected by the *Z* value is tabulated in Table 4.

3.2. Regional climate model and data

3.2.1. Weather research and forecasting model (WRF)

Developed at the National Center for Atmospheric Research (NCAR) in the USA, the WRF model is suitable for a broad spectrum of applications across scales ranging from meters to thousands of kilometers. The model incorporates advanced numeric and data-assimilation techniques, a multiple nesting capability and numerous state-of-the-art physics options. The model has found wide applications in climate research and in weather forecasting. Additional information can be obtained from: <http://www.wrf-model.org>.

3.2.2. Providing regional climates for impacts studies (PRECIS)

PRECIS, developed by the Hadley Centre of the UK MetOffice, is another regional climate modelling tool that can be run over any

Table 4
Trend detected for *Z* value at significant level $\alpha = 0.05$.

<i>Z</i>	Trend detected
$Z > 1.96$	Significant increase
$0 < Z \leq 1.96$	Insignificant increase
$-1.96 \leq Z < 0$	Insignificant decrease
$Z < -1.96$	Significant decrease

area of the globe on a relatively inexpensive, fast personal computer to provide regional climate information for impacts studies. The RCM PRECIS is based on the atmospheric component HadAM3P of the GCM HadCM3 with substantial modifications to the model physics. *The model can, however, only be run at horizontal resolutions of either 0.44° (50 km) or 0.22° (25 km).* The PRECIS version 1.9.3 was used in this study. The PRECIS model has been documented in detail by Jones et al. (2004) and is available from the PRECIS website: <http://precis.metoffice.com/>.

3.2.3. Reanalysis ERA-interim

The Reanalysis data used was the European Re-Analysis Interim dataset (Dee et al., 2011), referred to in this study as 'ERA'. The data have a spatial resolution of 1.5° longitude × latitude. Unlike other reanalysis data, ERAI only covers the recent period from 1989 to present in preparation for the next generation extended reanalysis to replace the older version ERA40. More information can be found in <http://www.ecmwf.int/research/era/do/get/era-interim>.

The lateral boundaries of the ERA-Interim reanalyses were used to drive both the WRF and PRECIS models in this study, at a horizontal model spatial resolution of 25 km. The simulations of WRF and PRECIS, each driven by ERA-Interim reanalyses, are referred to in this paper as WRF/ERA and PRE/ERA, for simple reading. The data from the PRECIS model, at the time of this study, was available only from 1989 to 2005. To match this period, data from the WRF model was also considered over the 1990 to 2005 period so that a common 16 year period can be taken from both models. It is for this data limitation, a longer period of 30 years could not be considered.

3.2.4. Gridded observation data

Two gridded observational datasets are used in this study for comparison of the RCMs WRF and PRECIS simulations: The Asian Precipitation Highly Resolved Observational Data Integration Towards Evaluation of water resources data (APHRODITE, referred to in this paper as 'APH') and the Tropical Rainfall Measuring Mission (referred to as 'TRMM').

The APH data was developed by the Research Institute for Humanity and Nature and Meteorological Research Institute of Japan. This dataset provides 0.25° resolution information on rainfall and surface temperature over the monsoon Asia on a daily time scale for long period 1961–2007. This was created primarily with data obtained from a rain gauge observation network. The basic algorithm was adopted in Xie (2007). More information can be found at the web link at: <http://www.chikyuu.ac.jp/precip/> and from Yatagai et al. (2012).

The TRMM provides information on tropical and subtropical precipitation (GES DISC, 2014). TRMM provides rainfall information from different satellite merged products from 1998 onwards until present. The monthly product TRMM 3B43 was used in this study. The version 3B43 has a monthly temporal resolution and a 0.25° × 0.25° spatial resolution. The spatial coverage extends from 50°S to 50°N and 0° to 360°E.

In this study, APH data which have a longer record was used to compare against both the station data and RCMs over the common period 1990–2005. On the other hand, TRMM with a recent satellite record was used for evaluations from 1999 onwards, to assess drought events.

3.2.5. Station data

There are 13 rainfall and meteorological stations over the study region. Monthly rainfall station data, which are spatially distributed all over the region, were collected. The spatial distribution of the rainfall stations are displayed in Fig. 1 and the details of these 13 stations are tabulated in Table 1. These data were obtained from the Institute of Meteorology, Hydrology and Envi-

ronment (IMHEN), under the Ministry of Natural Resources and Environment, Vietnam. These data were used for benchmarking model performance on a local scale. For simple reading, these are referred to as 'STA' data.

3.3. Methodology

The SPI was calculated for meteorological drought using monthly precipitation (both station data and gridded observations) for the period 1990–2005 at 13 rainfall stations in both temporal and spatial scales. The drought characteristics and their statistical properties (number of drought, frequency and deficit/severity) proposed by Yevjevich (1967) at different stations are computed based on the station data and on the bi-linearly interpolated (to the station point) gridded data. The spatial distribution of severe drought events was calculated for gridded observation data (APH & TRMM) as a benchmark to compare the RCMs' results. The MMK trend test was applied for the SPI indices for both station and gridded datasets to assess drought trends.

4. Results

4.1. Assessing drought in temporal scale

4.1.1. Drought events

The value of SPI from the 5 different datasets (STA, APH, TRMM, WRF/ERA, PRE/ERA) was calculated for all rainfall stations and for rainfall averaged over the study region. Due to space constraints, only SPI calculated for regional average is displayed in Fig. 2. SPI for all single stations shows similar trends as the average. In Fig. 2, the value of SPI higher than (lower than) 0 is indicated as blue color (red color), representing the wet and dry period, respectively. It needs to be stressed here that the drought event begins when the SPI first falls below zero and ends with the positive value of SPI following a value of -1.0 or less (McKee et al., 1993).

In Fig. 2a, the STA shows that the year 1998 exhibits extreme drought with a very high SPI value of -2 . This is in line with the study by Nguyen (2005) as the drought in 1998 was caused after the strong El Niño hit the region in 1997. The APH, in Fig. 2b, also indicates similar trends of severe drought in 1998. The WRF/ERA (Fig. 2d) shows moderate to severe drought during 1998 and exhibits additional drought patterns over next 2 years. The PRE/ERA (Fig. 2e) also indicates moderate to near-severe drought in 1998 (refer the drought severity scale in the figure).

However, prior to the 1998 extreme drought, there were several moderate ($-1.5 < \text{SPI} < -1$) to severe drought ($-2 < \text{SPI} < -1.5$) events as seen from STA and APH data over the period 1991 to mid of 1996 (except 1994). WRF/ERA was able to capture this signature. PRE/ERA was able to capture only 1 event in 1995. During the subsequent years after 1998, STA and APH datasets show severe to extreme drought over 2002–2005 (except 2004) with an extreme event in 2005. The TRMM (Fig. 2c) with shorter record (1998 on ward) also captured this signature. Both RCMs, WRF and PRECIS, were able to simulate the extreme drought in 2005. The WRF/ERA was successful in observing the wet event in 1994 and 2004, as seen in both STA and APH datasets. Overall, during the study period of SPI calculation 1990–2005, there are 4 events recorded by STA and APH, 5 events simulated by WRF/ERA and 3 events simulated by PRE/ERA (Table 5).

4.1.2. Drought Deficit and frequency

The Drought characteristics was also assessed by the Drought Deficit (DD) and drought frequency (DF) (Table 5). The Drought Deficit, which shows the magnitude of drought over the study period, was calculated as the summation of SPI value (negative value

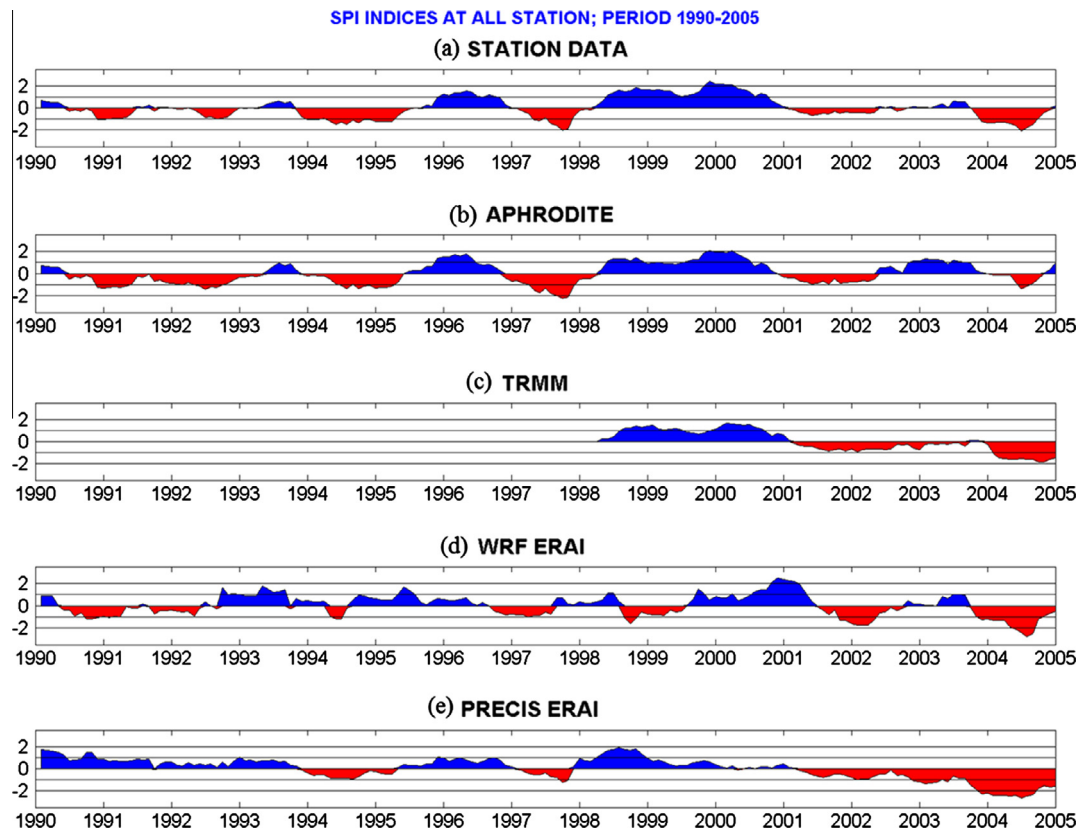


Fig. 2. SPI calculated for Kon Tum station using different datasets. (a) Station data, (b) APH, (c) TRMM, (d) WRF/ERA1 and (e) PRE/ERA1.

and unitless) for all drought period. The DF, which depicts the occurrence probability of drought for the study period, is the division of total duration of drought period (in months) with total number of months in the study period. Only the STA, APH and RCMs are shown as the TRMM with relatively shorter period is not considered for this purpose.

From Table 5, the model simulations WRF/ERA1 and PRE/ERA1 were able to generate similar drought characteristics as shown in STA and APH datasets, for the region average. The APH data, in spite of being gridded observation data (with same number of drought events), shows deviations when compared to STA data in both DD and DF. The DD for APH (−56.94) and PRE/ERA1 (−55.09) are the highest with respect to station data and similar trend was found for APH DF at 0.32 with respect to 0.26 of station data. The DF calculated by WRF/ERA1 is equal to that observed by STA at 0.26 and WRF/ERA1 also has closer DD value to STA than APH and PRE/ERA1. This suggests that RCMs' simulations were able to reproduce the drought characteristics over this region to a good extent.

4.2. Assessing severe drought in spatial scale

In order to investigate the spatial variations of drought, the two severe to extreme drought events (May 1998 and May 2005),

Table 5
Characteristics of drought events for all stations in Central Highland, period 1990–2005.

Characteristics	STA	APH	WRF/ERA1	PRE/ERA1
Number of drought events	4	4	5	3
Deficit	−45.63	−56.94	−53.39	−55.09
Frequency	0.26	0.32	0.26	0.21

chosen from two El Niño periods, are plotted in Fig. 3 (without TRMM) and Fig. 4 (with TRMM). The ENSO 1997 induced 1998 drought are shown spatially by STA and different gridded datasets in Fig. 3 for May 1998 (the driest month in 1998). Only APH and the RCM results are displayed spatially. As the STA data is point scale, it is indicated by a triangle (red inverted triangle represents drought and blue triangle represents wetness, the deficit scale is represented by the different sizes of the triangles, as indicated in the figure legend). For drought in May 2005, the TRMM is added for comparison (Fig. 4).

The figures indicate that severe to extreme drought occur over most of the regions (STA and RCMs) in 1998. In STA (Fig. 3a), only Da Lat station, which is a low lying area, did not suffer from drought, while all other stations show decreasing trends. The extreme drought was found occurring in the north. WRF/ERA1 was able to capture the wetness of Da Lat at the southeastern side of the study region (Fig. 3c). APH (Fig. 3b) agreed with most of the STA with the extreme drought in the northeastern side. PRE/ERA1 show reversed trends in comparison with APH and STA for the northern parts of the domain (Fig. 3d).

The 2005 drought is displayed in Fig. 4. STA and all datasets show the same negative values of SPI, indicating drought all over the region. However, the intensity of drought is different among these. STA, APH and TRMM display severe drought in the central parts and moderate drought toward the north and south region (Fig. 4a–c). WRF/ERA1 indicates extreme drought in the central region and severe drought over the eastern side (Fig. 4d). PRE/ERA1 shows extreme drought over the full domain (Fig. 4e).

4.3. Assessing drought frequency distribution

The drought frequency distribution is investigated for all stations and over the Central Highland region (Fig. 5). The SPI fre-

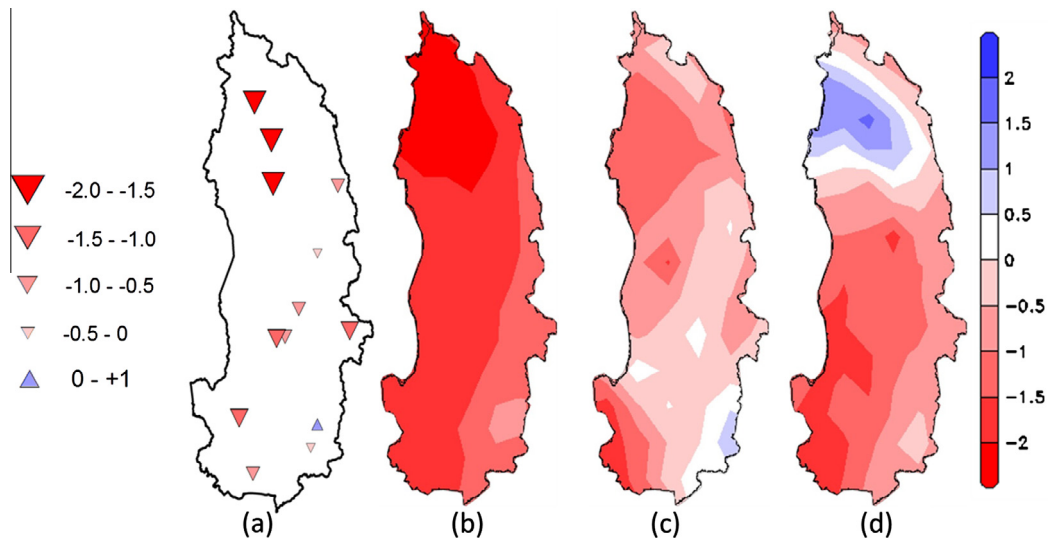


Fig. 3. Spatial distribution of SPI drought for May 1998 over different datasets: (a) STA, (b) APH, (c) WRF/ERA-Interim and (d) PRE/ERA-Interim.

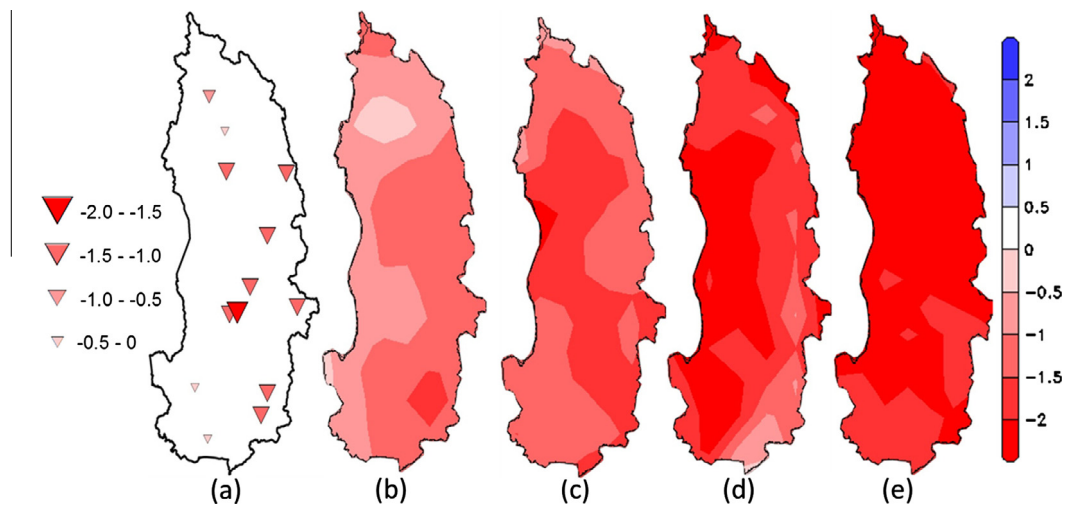


Fig. 4. Spatial distribution of SPI drought for May 2005 over different datasets: (a) STA, (b) APH, (c) TRMM, (d) WRF/ERA-Interim and (e) PRE/ERA-Interim.

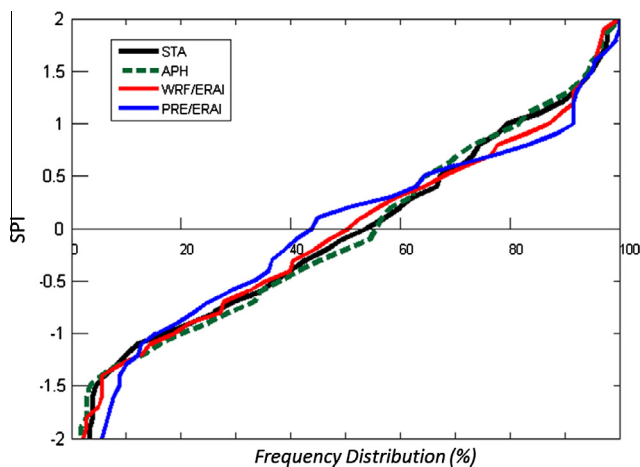


Fig. 5. Frequency distribution of SPI index for all datasets average for Central Highland, period 1990–2005.

quency plot shows a good agreement between STA, APH and the RCMs. TRMM dataset is not shown here due to its relatively shorter

record. The moderate to severe drought ($-2 < \text{SPI} < -1$) holds about 20% of the whole duration for all datasets. There is still discrepancy on SPI between STA and APH dataset, although the APH is a gridded product. When compared to the SPI trend of STA and APH data, the PRE/ERA-Interim underestimates mild drought by about 5–10%. The WRF/ERA-Interim agrees well with the observations.

4.4. Trend test using Modified Mann–Kendall for Drought

The Modified Mann–Kendall trend test for SPI index for all datasets is displayed in Fig. 6 and the metrics are shown in Table 4. In Fig. 6a, the MMK was calculated at all stations in the region and displayed in the map (grey and coloured triangles). The blue (red inverted) triangle indicates ‘significant’ increasing (decreasing) trend. The insignificant trend is displayed as upright/inverted triangles, in grey color. The MMK for the gridded datasets is displayed in red–white–blue color with red (blue) color showing decreasing (increasing) trend. The dark red/blue color represents significant decrease/increasing trend of SPI while the light red/blue¹ color indicate insignificant increasing trend, shown in Fig. 6.

¹ For interpretation of color in Fig. 6, the reader is referred to the web version of this article.

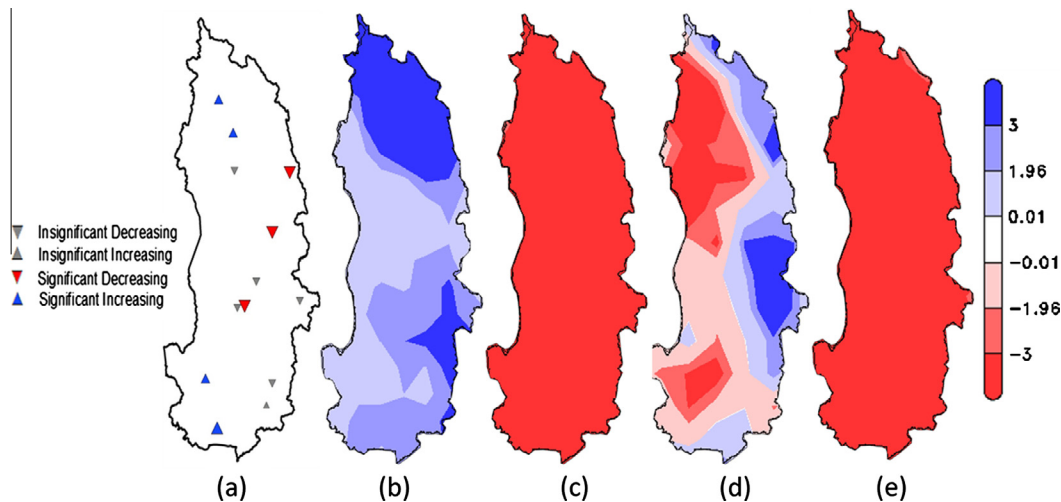


Fig. 6. Modified Mann-Kendall trend test for SPI: (a) STA, (b) APH, (c) TRMM, (d) WRF/ERA-I and (e) PRE/ERA-I.

As seen in Fig. 6a for STA dataset, out of 13 rainfall stations, 4 stations (Dak To, Kon Tum, Dak Nong, Bao Loc) show significant SPI increasing (wetter) trend, 3 stations (An Khe, Ayunpa, Eakmat) show significant decreasing trends (drier), 5 stations (Pleiku, Buon Ho, Buon Me Thuot, Mdrack, Da Lat) indicate insignificant decreasing trend and 1 station (Lien Khuong) exhibits insignificant increasing trend. The locations of 4 stations which showed significant wet trends are located at high altitudes compared to 3 stations that have significant dry trend that are located at altitudes. This is evident from the topography map of Fig. 1. It can be implied that the higher (lower) altitude regions showed a wetter (drier) tendency. Overall, the eastern side of the study domain exhibited drier tendencies with both significant and insignificant trend produced by the MMK trend test.

However, both the gridded observation data (APH, TRMM) and the downscaled data (WRF, PRECIS) do not agree with these patterns observed in the station data. Obviously, in Fig. 6c and e, the TRMM and PRE/ERA-I indicated significant decreasing trend of SPI over the whole region, whilst the APH (Fig. 6b), on the other hand showed an increasing trend with the significant value over the northern and southeastern part of the domain. The WRF/ERA-I (Fig. 6d) alone shows mixed trends (significant and insignificant value of both wet and dry index) as the station data. However, the WRF/ERA-I spatial distributions of wet and dry regions do not match with the station data. Hence, the Modified Mann-Kendall trend test for the station data has mixed trends and the trends follow the topography of the domain. It does not yield a clear conclusion on the assessment of the wet/dry trends because of the existence of data differences. It is likely that this could be due to the short study period for 16 years that might not be enough for the MMK trend test.

5. Conclusions

This paper studied the drought conditions of Central Highland, Vietnam based on the SPI index. Different datasets were used in this study: station data (STA), gridded observation data from rain gauge (APH), merged satellite product (TRMM) and regional climate models (WRF and PRECIS), driven by reanalysis data ERA-I. Few drought characteristics were analyzed based on the number of drought events, Drought Deficit and drought frequency to compare the historical drought over Central Highland. The results can be summarized as: (1) All gridded and RCM data were able to capture the SPI index in temporal scales for all 13 stations over the

study region. (2) Gridded and RCM data successfully captured the spatial structure of the SPI index that indicated drought over the study region during the severe drought events of 1998 and 2005. (3) The Modified Mann-Kendall trend for SPI shows mixed trend for station and one of the RCMs, but the other data did not yield any conclusive results on the trends.

Given these results, analyzing future drought using the RCM results of downscaled future climates under different emission scenarios and pathways would be immensely helpful for adaptation and policy decisions and will be a continued exercise of this study. However, primarily robust observations could alleviate the uncertainties that arise in computing different statistical metrics as the RCM validations are done against observations. Hence, the quality of observations is crucial, especially over regions of complex topography. This would be the first step to be addressed when assessing drought and its trends over historical periods, before a detailed study using climate model data can be entertained. Yet, the study has highlighted the usefulness of applying climate model data to assess impacts which could be immensely useful over regions where data are scarce. In that sense, the use of RCM as proxies to observed data can be emphasized.

References

- American Meteorological Society (AMS), 2013. Drought: an information statement of the American Meteorological Society. *Bull. Am. Meteorol. Soc.* 94 (12), 1932–1936.
- Belayneh, A., Adamowski, J., 2012. Standard Precipitation Index drought forecasting using neural networks, wavelet neural networks, and support vector regression. *Appl. Comp. Intell. Soft Comp.* Article ID 794061, 1–13. Doi: 10.1155/2012/794061.
- Birsan, M.V., Molnar, P., Burlando, P., Pfaundler, M., 2005. Streamflow trends in Switzerland. *J. Hydrol.* 314, 312–329.
- Bordi, I., Sutera, A., 2007. Drought monitoring and forecasting at large-scale. In: Rossi, G., Vega, T., Bonaccorso, B. (Eds.), *Methods and Tools for Drought Analysis and Management*. Springer, New York, NY, USA, pp. 3–27.
- Dao, X.H., 2002. *Drought and Its Mitigation Measures*. Agricultural Publishing House, Hanoi, Vietnam, p. 188 (in Vietnamese).
- Daufresne, M., Lengfellner, K., Sommer, U., 2009. Global warming benefits the small in aquatic ecosystems. *Proc. Natl. Acad. Sci. USA* 106 (31), 12788–12793.
- de Martonne, E., 1926. Une nouvelle fonction climatologique: L'Indice d'aridité. *La Meteorol.* 2, 449–458.
- Dee, D.P., Uppala, S.M., Simmons, A.J., Berrisford, P., Poli, P., Kobayashi, S., Andrae, U., Balmaseda, M.A., Balsamo, G., Bauer, P., Bechtold, P., Beljaars, A.C.M., van de Berg, L., Bidlot, J., Bormann, N., Delsol, C., Dragani, R., Fuentes, M., Geer, A.J., Haimberger, L., Healy, S.B., Hersbach, H., Hólm, E.V., Isaksen, I., Kållberg, P., Köhler, M., Matricardi, M., McNally, A.P., Monge-Sanz, B.M., Morcrette, J.J., Park, B.K., Peubey, C., de Rosnay, P., Tavolato, C., Thépaut, J.N., Vitart, F., 2011. The ERA-Interim reanalysis: configuration and performance of the data assimilation system. *Quar. J. R. Met. Soc.* 137, 553–597.

- Douglas, E.M., Vogel, R.M., Kroll, C.N., 2000. Trends in floods and low flows in the United States: impact of spatial correlation. *J. Hydrol.* 240, 90–105.
- GES DISC (Goddard Earth Sciences – Data and Information Services Centre). http://disc.gsfc.nasa.gov/precipitation/trmm_intro.shtml (access 18.04.14).
- Gocic, M., Trajovic, S.P., 2013. Analysis of precipitation and drought data in Serbia over the period 1980–2010. *J. Hydrol.* 494 (3–4), 32–42.
- Guttman, N.B., 1999. Accepting the Standardized Precipitation Index: a calculation algorithm. *J. Am. Water Resour. Assoc.* 35 (2), 311–322.
- Hamed, K.H., Rao, A.R., 1998. A modified Mann-Kendall trend test for autocorrelated data. *J. Hydrol.* 204, 182–196.
- Heim Jr., R.R., 2002. A review of twentieth-century drought indices used in the United States. *Bull. Am. Meteorol. Soc.* 83, 1149–1165.
- IPCC, 2014. Climate change 2014: impacts, adaptation, and vulnerability. Part A: Global and sectoral aspects. In: Field, C.B., Barros, V.R., Dokken, D.J., Mach, K.J., Mastrandrea, M.D., Bilir, T.E., Chatterjee, M., Ebi, K.L., Estrada, Y.O., Genova, R.C., Girma, B., Kissel, E.S., Levy, A.N., MacCracken, S., Mastrandrea, P.R., White, L.L. (Eds.), Contribution of Working Group II to the Fifth Assessment Report of the Intergovernmental Panel on Climate Change. Cambridge University Press, Cambridge, United Kingdom and New York, NY, USA.
- Jones, R.G., Noguera, M., Hassell, D.C., Hudson, D., Wilson, S.S., Jenkins, G.J., Mitchell, J.F.B., 2004. Generating high resolution climate change scenarios using PRECIS. Technical Report. Hadley Centre, UK MetOffice, p. 40.
- Kendall, M.G., 1975. *Rank Correlation Methods*, fourth ed. Charles Griffin, London.
- Lyon, B., Lareef, Z., Vidhura, R., Zeenas, Y., 2009. Finescale evaluation of drought in a tropical setting: case study in Sri Lanka. *J. Appl. Meteor. Climatol.* 48, 77–88.
- Mann, H.B., 1945. Nonparametric tests against trend. *Econometrica* 13, 245–259.
- McKee, T.B., Doesken, N.J., Kleist, J., 1993. The relationship of drought frequency and duration to time scales. In: Proc. 8th Conf. on Appl. Clim. Am. Meteorol. Soc. Boston, Massachusetts, pp. 179–184.
- Mishra, A.K., Singh, V.P., 2011. Drought modelling – a review. *J. Hydrol.* 403, 157–175.
- Nguyen, Q.K., 2005. Evaluating drought situation and analysis drought events by drought indices. National Project Drought Research Forecast Centre South Central Highland Vietnam Constructing Prevent Solution, 209 (in Vietnamese).
- Nguyen, D.T., Cintia, U., Dan, R., 2007. Relationship between the tropical Pacific and Indian Ocean sea-surface temperature and monthly precipitation over the Central Highlands, Vietnam. *Short Commun., Int. J. Climatol.* 27, 1439–1454.
- Novotny, E.V., Stefan, H.G., 2007. Stream flow in Minnesota: indicator of climate change. *J. Hydrol.* 334 (3–4), 319–333.
- Ntale, H.K., Gan, T.Y., 2003. Drought indices and their application to East Africa. *Int. J. Climatol.* 23, 1335–1357.
- Obasi, G.O.P., 1994. WMO's role in the international decade for natural disaster reduction. *Bull. Am. Meteorol. Soc.* 75 (9), 1655–1661.
- Palmer, W.C., 1965. Meteorologic drought. US Department of Commerce, Weather Bureau, Research Paper No. 45, p. 58.
- Partal, T., Kahya, E., 2006. Trend analysis in Turkish precipitation data. *Hydrol. Proc.* 20, 2011–2026.
- Ped, D.A., 1975. On indicators of droughts and wet conditions. *Proc. USSR Hydrometeor. Cent.* 156, 19–39 (in Russian).
- Raziei, T., Saghafian, B., Paulo, A.A., Pereira, L.S., Bordi, I., 2009. Spatial patterns and temporal variability of drought in western Iran. *Water Resour. Manage* 23 (3), 439–455.
- Tabari, H., Talaei, H.P., 2011a. Analysis of trends in temperature data in arid and semi-arid regions of Iran. *Glob. Planet. Change* 79 (1–2), 1–10.
- Tabari, H., Talaei, H.P., 2011b. Temporal variability of precipitation over Iran: 1966–2005. *J. Hydrol.* 396 (3–4), 313–320.
- Tabari, H., Abghari, H., Talaei, H.P., 2012. Temporal trends and spatial characteristics of drought and rainfall in arid and semiarid regions of Iran. *Hydrol. Process.* 26 (22), 3351–3361.
- Tran, V.L., 1999. Relation between forest ecosystem and Hydro-climate in the Central Highland of Vietnam. Report of National Program on Forest Inquire and Planning of the Period 1995–2000. Ins. of Forest Investigat. Plann., Hanoi, p. 145 (in Vietnamese).
- US EPA. Natural disasters. <http://epa.gov/naturaldisasters/index.html> (access September 2014).
- Vu, T.H., Ngo, D.T., Phan, V.T., 2013. Evolution of meteorological drought characteristics in Vietnam during the 1961–2007 period. *Theor. Appl. Climatol.* Doi: 10.1007/s00704-013-1073-z.
- World Meteorological Organization (WMO), 2009. Experts agree on a universal drought index to cope with climate risks. WMO Press Release No. 872. http://www.wmo.int/pages/prog/wcp/agm/meetings/wies09/documents/872_en.pdf (accessed 2014).
- Wu, H., Hayes, M.J., Wilhite, D.A., Svoboda, M.D., 2005. Effect of the length of record on the Standardized Precipitation Index calculation. *Int. J. Climatol.* 25, 505–520.
- Xie, P., Yatagai, A., Chen, M., Hayasaka, T., Fukushima, Y., Liu, C., Yang, S., 2007. A gauge-based analysis of daily precipitation over East Asia. *J. Hydrometeor.* 8, 607–627.
- Yatagai, A., Kamiguchi, K., Arakawa, O., Hamada, A., Yasutomi, N., Kitoh, A., 2012. APHRODITE: constructing a long-term daily gridded precipitation dataset for Asia based on a dense network of rain gauges. *Bull. Am. Meteorol. Soc.* 93, 1401–1415.
- Yevjevich, V., 1967. An objective approach to definitions and investigations of continental hydrologic drought. *Hydrol. Paper No. 23*, Colorado State Univ., Fort Collins, Colo.
- Yusof, F., Mean, F.H., Suhaila, J., Yusop, Z., Yee, K.C., 2014. Rainfall characterisation by application of Standardized Precipitation Index (SPI) in Peninsular Malaysia. *Theor. Appl. Climatol.* 115, 503–516.
- Zhang, Q., Li, J., Singh, V.P., Bai, Y., 2012. SPI-based evaluation of drought events in Xinjiang, China. *Nat. Hazard* 64, 481–492.
- Zhang, L., Fraedrich, K., Zhu, X., Sielmann, F., Zhi, X., 2014. Interannual variability of winter precipitation in Southeast China. *Theor. Appl. Climatol.* Doi: 10.1007/s00704-014-1111-5.